Impact of Modular Total Absorption Spectrometer measurements of β decay of fission products on the decay heat and reactor $\bar{\nu}_e$ flux calculation

A. Fijałkowska,[1,2,3,*] M. Karny,[1,4,5] K. P. Rykaczewski,[4] B. C. Rasco,[3,4,5,6] R. Grzywacz,[3,4,5] C. J. Gross,[4] M. Wolińska-Cichocka,[7,4,5] K. C. Goetz,[3,8] D. W. Stracener,[4] W. Bielewski,[1] R. Goans,[9] J. H. Hamilton,[10] J. W. Johnson,[4] C. Jost,[3] M. Madurga,[3] K. Miernik,[1,4] D. Miller,[3] S. W. Padgett,[3] S. V. Paulauskas,[3] A. V. Ramayya,[10] and E. F. Zganjar[6]

[1]*Faculty of Physics, University of Warsaw, PL-02-093 Warsaw, Poland*
[2]*Department of Physics and Astronomy, Rutgers University, New Brunswick, New Jersey 08903, USA*
[3]*Department of Physics and Astronomy, University of Tennessee, Knoxville, Tennessee 37966, USA*
[4]*Physics Division, Oak Ridge National Laboratory, Oak Ridge, Tennessee 37831, USA*
[5]*JINPA, Oak Ridge National Laboratory, Oak Ridge, Tennessee 37831, USA*
[6]*Department of Physics and Astronomy, Louisiana State University, Baton Rouge, Louisiana 70803, USA*
[7]*Heavy Ion Laboratory, University of Warsaw, PL-02-093 Warsaw, Poland*
[8]*CIRE Bredesen Center, University of Tennessee, Knoxville, Tennessee 37966, USA*
[9]*Oak Ridge Associated Universities, Oak Ridge, Tennessee 37831, USA*
[10]*Department of Physics and Astronomy, Vanderbilt University, Nashville, Tennessee 37235, USA*

We report the results of a β-decay study of fission products ^{86}Br, ^{89}Kr, ^{89}Rb, ^{90gs}Rb, ^{90m}Rb, ^{90}Kr, ^{92}Rb, ^{139}Xe, and ^{142}Cs performed with the Modular Total Absorption Spectrometer (MTAS) and on-line mass-separated ion beams. These radioactivities were assessed by the Nuclear Energy Agency as having high priority for decay heat analysis during a nuclear fuel cycle. We observe a substantial increase in β feeding to high excited states in all daughter isotopes in comparison to earlier data. This increases the average γ-ray energy emitted by the decay of fission fragments during the first 10 000 s after fission of ^{235}U and ^{239}Pu by approximately 2% and 1%, respectively, improving agreement between results of calculations and direct observations. New MTAS results reduce the reference reactor $\bar{\nu}_e$ flux used to analyze reactor $\bar{\nu}_e$ interaction with detector matter. The reduction determined by the *ab initio* method for the four nuclear fuel components, ^{235}U, ^{238}U, ^{239}Pu, and ^{241}Pu, amounts to 0.976, 0.986, 0.983, and 0.984, respectively.

Beta decay is one of the fundamental transformations of atomic nuclei. The experimental β-decay data accessible through data-evaluation centers, e.g., [1], are important sources of information used in research and applications. β-decay rates are an essential component of the astrophysical r-process calculation, determining final nuclear abundance [2–5]. Decay schemes of fission products are used to calculate the decay heat release in nuclear reactors as well as the reactor $\bar{\nu}_e$ flux used to study fundamental $\bar{\nu}_e$ properties [6–9]. The precision of existing global models describing β-decay properties strongly depends on the completeness and quality of available experimental data [10,11].

Experimental decay schemes based on high-resolution but low-efficiency measurements are burdened with systematic error due to the inability to detect numerous weak β transitions feeding highly excited states in the daughter nucleus (the pandemonium effect) [12]. The most comprehensive data are obtained by exploring the β decay with total absorption spectroscopy; these are very efficient systems that measure the β strength over the entire decay energy window [13,14]. In this Letter we present results of total absorption β-decay studies of nine fission products

important for decay heat analysis [6] and their impact on the decay heat and reactor $\bar{\nu}_e$ spectrum calculation.

Decay heat is defined as the γ, β, and β-delayed neutron energy released during the radioactive decay of fission products. Decay heat, along with the kinetic energy of fission fragments and the kinetic energy of prompt neutrons and γ rays, is one of the basic components contributing to the total energy release in nuclear power plants. It is the only source of heat in the nuclear fuel rods after reactor shutdown [6]. Knowledge of the amount and form of energy emitted in the radioactive decays of fission products is critical for the determination of safety procedures for nuclear power plant operation and for the cooling of nuclear fuel after an accidental or planned reactor shutdown. The durability of reactor construction materials depends on the detailed radiation exposure of these materials. Moreover, reliable knowledge of the decay heat contribution to the energy production is important for economic reasons, helping to improve reactor efficiency [6].

Decay heat calculations based on published experimental data lead to results inconsistent with direct observations. The differences are identified as arising from the underestimation

of the longer range γ-ray flux and overestimation of energy carried by electrons, which have a much shorter range [6,15]. These discrepancies are believed to be due to the incorrect or incomplete β-decay schemes of fission products, usually based on low-efficiency measurements. This leads to the underestimation of the average γ-ray energy and overestimation of the β energy. The solution is to measure the β decay of fission products using high-efficiency systems like total absorption spectrometers (TASs) [16–19]. The assessment performed by the Nuclear Energy Agency (NEA) under the auspices of the Organization for Economic Cooperation and Development (OECD) provided a list of fission products important for the analysis of decay heat, and recommended measurements using the total absorption technique [6]. This NEA OECD list provided a guidance for a number of TAS measurements, see [13,18]. We present the results of total absorption measurements including seven fission products from the NEA OECD list, with four assessed as priority 1.

Reliable measurements of the β decay of fission products are also important to properly estimate the reference number of reactor $\bar{\nu}_e$ interactions with matter [8,20]. Nuclear reactors are powerful sources of $\bar{\nu}_e$, which makes them extremely useful in the study of fundamental $\bar{\nu}_e$ properties [7]. Recently, a number of large-scale measurements of mixing angle θ_{13} using the reactor $\bar{\nu}_e$ were performed, at Double Chooz [21], Daya Bay [9,22,23], and RENO [24]. It was observed that the number of detected reactor $\bar{\nu}_e$ interactions is about 0.95(2) of the expected number of events. This disparity has been dubbed the "reactor antineutrino anomaly" [7,23]. The existence of sterile neutrinos has been put forward to explain the discrepancy [7]. Here we point to a systematic error made when calculating the reference reactor $\bar{\nu}_e$ spectra [25]. Incomplete information about the β-decay schemes of fission products tends to underestimate the probability of β transitions feeding high-excited states, which artificially shifts the calculated $\bar{\nu}_e$ flux to higher energies. This causes an overestimation of the predicted number of detected $\bar{\nu}_e$. Studies of the β decay of fission fragments using total absorption detectors find a more accurate $\bar{\nu}_e$ distribution and, consequently, a better estimate of the number of expected interactions with matter. Radioactive nuclei important for decay heat estimation are also critical for the calculation of the number of reactor $\bar{\nu}_e$ interactions with matter, since these nuclei are created abundantly in nuclear reactors and contribute substantially to the overall γ, β, and $\bar{\nu}_e$ flux.

The experiments were performed at the Holifield Radioactive Ion Beam Facility at the Oak Ridge National Laboratory [26]. A 40-MeV proton beam irradiated a ^{238}UCx target that was close-coupled to an ion source [27]. Three types of ion sources were used—a plasma ion source, a surface ionization ion source, and a LaB_6 source. Fission products were mass selected by means of electromagnetic on-line separation. Nuclides of a given mass were

implanted onto a tape that transported the radioactive samples into the center of the Modular Total Absorption Spectrometer (MTAS) where they were measured; they then moved away to a shielded chamber. Signals from the MTAS and complementary detectors were processed using Pixie16 modules, Rev.D, XIA LLC [28–30]. The MTAS detector consists of 19 hexagonal-shaped NaI(Tl) crystals arranged in a honeycomb structure. Two segmented 1-mm-thick silicon β detectors in the center of the MTAS provided β trigger signals [19].

A Monte Carlo simulation code was developed by means of the GEANT4 toolkit version 4.9.4.p02 [31] to reproduce the response function of MTAS for γ and β radiation. The detector model was verified with the use of several calibration sources [19]. In brief, two basic types of experimental spectra were made to aid the analysis of the β-decay scheme. The β-gated sum of all add-up signals from 19 detector modules (TAS spectrum) is typically compared to the respective simulations following existing data base entry and used to establish β intensities. However, the analysis of individual spectra of all MTAS modules enabling determination of γ-γ coincidences also substantially aids the analysis of γ lines emitted after β transitions. Based on the GEANT4 detector model, analogous spectra were calculated using decay schemes published in the Evaluated Nuclear Structure Data File (ENSDF) database [1]. Missing high-energy levels were restored by adding bins every 100 keV starting from a minimum energy E_{min}, determined individually for each nucleus and ending with energy equal to $Q_\beta - 300$ keV. The maximum entropy method was used to fit β intensities including ground-state feeding [32]. Details of the analysis are given in [19,20].

Figure 1 shows, as an example, a comparison of the experimental data, simulated ENSDF spectra, and simulated MTAS spectra for ^{139}Xe [33]. The major changes in the decay scheme were the reduction of the ground-state
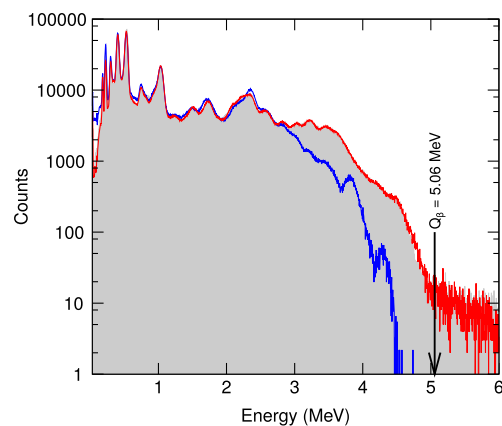

FIG. 1.   Experimental total energy deposited in MTAS detector emitted in the decay of ^{139}Xe (grey) compared with the simulated detector response based on ENSDF data (blue) and the simulated detector response based on the final result of the analysis (red).
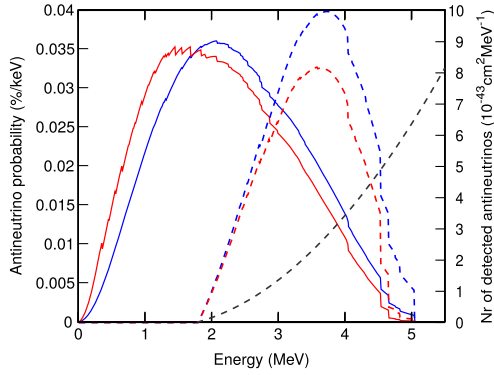
FIG. 2. Comparison of the $\bar{\nu}_e$ distribution emitted in the decay of ^{139}Xe, calculated based on decay scheme published in the ENSDF database [1] (blue, solid line) and the results of MTAS measurements (red solid line). The black dashed curve shows the shape of the inverse β-decay cross section [34]. Blue and red dashed lines show the product of the $\bar{\nu}_e$ energy distribution and the inverse β-decay cross section for ENSDF and MTAS data, respectively.

feeding from 15(10)% to 2(1)% and new β-fed levels above 3.6 MeV. β-transition intensities to levels above 2.5 MeV are increased by over 15%.

The new decay schemes were used to determine the average γ-ray energy, $\overline{E_\gamma}$, the average β energy, $\overline{E_\beta}$, and the probability of detecting an $\bar{\nu}_e$ emitted during the decay. For this purpose $\bar{\nu}_e$ energy spectra were calculated assuming an allowed β shape and zero recoil energy of the daughter nucleus. The average probability of detecting an $\bar{\nu}_e$, expressed in cm^2 units, is an integral of a product of the obtained spectra and the inverse β-decay cross section [34] The ^{139}Xe MTAS results for emitted and detected $\bar{\nu}_e$ are shown in Fig. 2. The steps in the $\bar{\nu}_e$ energy distribution results from the β^- spectrum shape, which has a finite intensity at $E_\beta = 0$ due to the Coulomb interaction with the

charge of the daughter nucleus. It represents the maximum energy of the $\bar{\nu}_e$ for a given β^- transition.

$\overline{E_\gamma}$ and $\overline{E_\beta}$ emitted in the β decay of ^{86}Br, ^{89}Kr, ^{89}Rb, ^{90gs}Rb, ^{90m}Rb, ^{90}Kr, ^{92}Rb, ^{139}Xe, and ^{142}Cs taken from the ENDF/B-VII.1 database and the MTAS measurements are presented in Table I. The most substantial changes were obtained for the decays of ^{89}Kr, ^{90}Kr, ^{139}Xe, and ^{142}Cs. The first three activities have the highest priority for reinvestigation in the NEA OECD report [6]. Indeed, decay schemes of these isotopes are incomplete and erroneous. For all of these nuclei except ^{86}Br, the ground-state feeding was significantly reduced: from 23(4)% to 11(1)% for ^{89}Kr, from 29(4)% to 7(1)% for ^{90}Kr, and from 56(5)% to 43(3)% for ^{142}Cs. The ^{90}Kr decay is an interesting case. Despite the small Q_β of 4.39(2) MeV, ^{90}Kr is a major contributor to the modification of reactor decay heat due to the high cumulative fission yield and the large reduction in the ground-state feeding.

Our results for ^{90gs}Rb and ^{90m}Rb reduce the β feeding to the first-excited 2^+ state in ^{90}Sr at 831.7 keV from 26(2)% and 15(4)% to 15(1)% and 5(1)%, respectively. The trend is consistent with the first TAS measurement according to which the first-excited state β feeding is 13.2% and 1.76% [37]. In addition, the result for ^{92}Rb is consistent with the recent total absorption measurement [38].

We use the MTAS results to determine the total change in the average γ-ray energy emitted from fission products of ^{235}U and ^{239}Pu irradiated by thermal neutrons, as well as the changes in the electromagnetic component of the decay heat. The fission yields used for this calculation were taken from the Joint Evaluated Fission and Fusion File (JEFF)-3.1 database [36]. The average γ-ray energy emitted by the decay of fission fragments during the first 10 000 s after fission increases by 2% and 1% for ^{235}U and ^{239}Pu, respectively. The calculated decay heat change for ^{235}U

TABLE I. The average γ-ray ($\overline{E_\gamma}$) and β ($\overline{E_\beta}$) energy emitted in the β decay of ^{86}Br, ^{89}Kr, ^{89}Rb, ^{90gs}Rb, ^{90m}Rb, ^{90}Kr, ^{92}Rb, ^{139}Xe, and ^{142}Cs taken from the ENDF/B-VII.1 database and determined based on MTAS measurement. Decay data such as half-life ($T_{1/2}$) and Q_β were taken from the ENDF/B-VII.1 database [35], while cumulative fission yield for ^{235}U fission ($Y_{cum} \times 100$) were taken from the JEFF-3.1 database [36]. σ symbol indicates the probability of detection $\bar{\nu}_e$ emitted in the decay. The rightmost column contains information about the priority given in the OECD report [6].

| Isotope	$T_{1/2}$ (s)	Q_β (MeV)	$Y_{cum} \times 100$ JEFF-3.1	$\overline{E_\gamma}$ (MeV)		$\overline{E_\beta}$ (MeV)		σ (10^{-43} cm^2)		Priority [6]
				ENDF	MTAS	ENDF	MTAS	ENSDF	MTAS	
^{86}Br	55.1(4)	7.633(3)	1.87(2)	3.3(2)	3.72(8)	1.9(3)	1.73(3)	2.6(8)	2.46(5)	1
^{89}Kr	189(2)	5.176(6)	4.43(6)	1.93(2)	2.24(8)	1.5(1)	1.25(4)	1.17(13)	0.77(4)	1
^{89}Rb	918(6)	4.496(5)	4.69(6)	2.24(6)	2.26(7)	0.97(5)	0.93(3)	0.42(3)	0.39(3)	
^{90gs}Rb	158(5)	6.587(8)	4.37(13)	2.27(4)	2.3(1)	1.9(1)	1.92(5)	3.3(3)	2.96(8)	
^{90m}Rb	258(4)	6.694(8)	1.4(2)	3.87(6)	4.0(2)	1.12(3)	1.1(1)	1.2(2)	0.56(15)	2
^{90}Kr	32.32(9)	4.39(2)	4.90(12)	1.32(4)	1.69(2)	1.4(1)	1.13(2)	0.68(8)	0.32(2)	1
^{92}Rb	4.48(3)	8.095(6)	4.83(14)	0.170(9)	0.385(8)	3.6(4)	3.57(7)	10.50(8)	10.1(2)	2
^{139}Xe	39.68(14)	5.06(2)	5.12(12)	1.02(2)	1.34(3)	1.8(2)	1.58(3)	1.8(3)	1.47(3)	1
^{142}Cs	1.684(14)	7.31(1)	2.9(3)	0.95(3)	1.72(5)	2.9(2)	2.48(9)	7.0(5)	5.1(2)	3
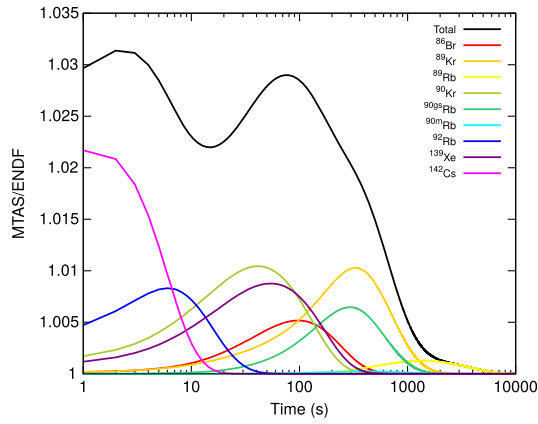
FIG. 3. The change of electromagnetic component of the decay heat calculated for ^{235}U + n_{th} fission. The different colors show the ratio of the decay heat calculated for MTAS and ENDF/B-VII.1 data (MTAS/ENDF) for individual nuclei. The black curve shows the total change.

is shown in Fig. 3. The plots show the ratio of the decay heat calculated for MTAS and ENDF/B-VII.1 data for each of the measured nuclei. The largest increases are seen in the first 5 s after fission and around 100 s after fission. The first increase is due to the large change in the average γ-ray energy emitted in the decay of ^{142}Cs ($T_{1/2} = 1.7$ s) and the second is from the combined contribution of ^{86}Br, ^{90}Kr, and ^{139}Xe decays. The increase in the electromagnetic component of the decay heat improves the agreement between calculated values and direct measurements [39], as shown in Fig. 4.

The second part of Table I contains information about the spectrum-averaged effective cross section for $\bar{\nu}_e$ interaction with matter (σ). The calculations are based on the decay schemes listed in the ENSDF database and the MTAS measurement. The largest change is observed for the decay of ^{142}Cs and ^{90m}Rb. ^{142}Cs was listed as one of the main

contributors to the high-energy part of the reactor $\bar{\nu}_e$ spectrum [40], while ^{90m}Rb is on the OECD list [6].

The total effect of the present MTAS measurements on the reactor $\bar{\nu}_e$ energy spectra emitted by reactor fuel components, calculated by the *ab initio* method, assuming that the system is in equilibrium [40,41], is shown in Fig. 5. The fission yields used to calculate the spectra in Fig. 5 are taken from the JEFF-3.1 database [36] and the decay schemes are taken from the ENSDF database. The discontinuities in the graph are due to changes of individual level feedings. Ground-state feedings are a prime example of this change and are marked in Fig. 5. The MTAS/ENSDF $\bar{\nu}_e$ energy ratio shows that the low-energy contribution is underestimated (below $\bar{\nu}_e$ energy 2 MeV) while the high-energy component is overestimated. Because the cross section for the $\bar{\nu}_e + p \rightarrow e^+ + n$ reaction is proportional to the square of $\bar{\nu}_e$ energy above the 1.8-MeV threshold [34], a shift towards the low energies reduces the number of $\bar{\nu}_e$ interactions with matter. The overall change in the number of $\bar{\nu}_e$ interactions for the four nuclear fuel components (MTAS/ENSDF) amounted to 0.976, 0.986, 0.983, and 0.984 for ^{235}U, ^{238}U, ^{239}Pu, and ^{241}Pu, respectively.

The reduction of reference antineutrino interactions is 0.979 for a typical nuclear fuel composition after 600 days of a reactor operation. The fuel composition is calculated using the ORIGEN program [42], assuming 4.8% fuel enrichment and 38 MW/MTU reactor power. This reduction in the expected number of reactor $\bar{\nu}_e$ interactions with matter highlights the need to complete β decay of fission products measured by total absorption technique [6] for the understanding of the reactor antineutrino anomaly phenomenon [7]. However, the large effect resulting from
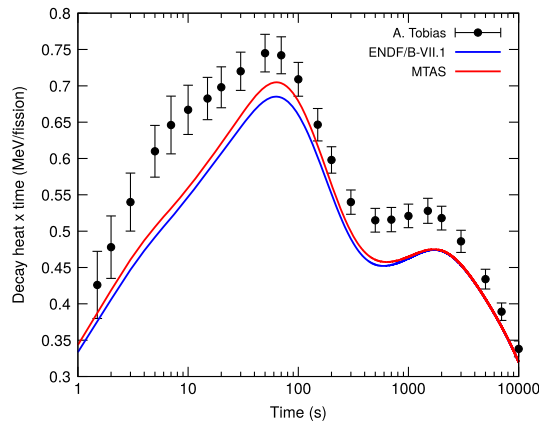

FIG. 4. Experimental electromagnetic component of the decay heat for ^{235}U fission (black points) [39] compared with the calculation based on ENDF/B-VII.1 data (blue) and ENDF/B-VII.1 corrected by MTAS results (red).
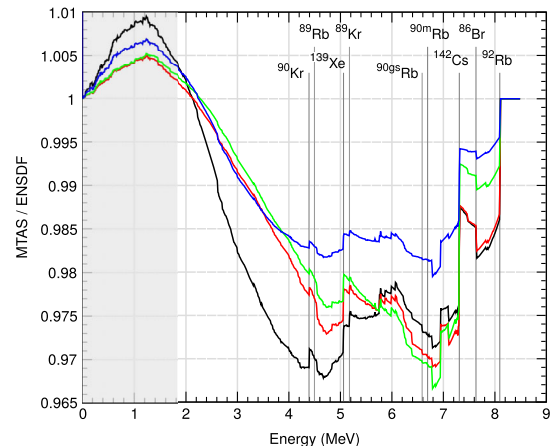

FIG. 5. Ratio of the calculated $\bar{\nu}_e$ energy distribution from the MTAS measurement and data contained in the ENSDF database, designated for the most important nuclear fuel types: ^{235}U (black), ^{238}U (blue), ^{239}Pu (red), and ^{241}Pu (green). The shaded area denotes energies below the inverse β-decay threshold. Vertical lines indicate the Q_β values of the measured nuclei.

P H Y S I C A L   R E V I E W   L E T T E R S

the MTAS study of ^{142}Cs [20], which was identified as only a priority-3 nucleus [6], calls for a reevaluation of the assessed priorities, and for respective future TAS measurements. In addition, as pointed out in [43], more refined analysis of β-decay schemes with respect to the allowed and first-forbidden transitions may further enhance the differences between TAS-modified reference $\bar{\nu}_e$ flux and its earlier estimations [25,44].

In this Letter we present the results of total absorption measurements of nine β-decaying fission products, of which seven nuclei are assessed as having high priority for decay heat analysis, as well as having significant contributions to the reactor $\bar{\nu}_e$ spectrum [6]. The measurements were performed using the Modular Total Absorption Spectrometer, presently the largest and most efficient total absorption spectrometer. MTAS results improve the agreement between calculated and measured decay heat increasing the average γ-ray energy emitted by the decay of fission fragments by 2% and 1% for ^{235}U and ^{239}Pu nuclear fuel components, respectively. These results also change the number of expected reactor $\bar{\nu}_e$ interactions with the detector matter (MTAS/ENSDF) for the four basic nuclear fuel components by 0.976, 0.986, 0.983, and 0.984 for ^{235}U, ^{238}U, ^{239}Pu, and ^{241}Pu, respectively. This indicates that the precision of reactor $\bar{\nu}_e$ spectra predictions is lower than specified [25], and demonstrates the importance of total absorption spectroscopy measurements for understanding the reactor antineutrino anomaly phenomenon.

---

[*]aleksandra.kuzniak@gmail.com

[1] http://www.nndc.bnl.gov/ensdf/.

[2] R. Surman, M. Mumpower, J. Cass, I. Bentley, A. Aprahamian, and G. McLaughlin, Eur. Phys. J. Web Conf. **66**, 07024 (2014).

[3] M. Madurga, R. Surman, I. N. Borzov, R. Grzywacz, K. P. Rykaczewski, C. J. Gross, D. Miller, D. W. Stracener, J. C. Batchelder, N. T. Brewer et al., Phys. Rev. Lett. **109**, 112501 (2012).

[4] G. Lorusso, S. Nishimura, Z. Y. Xu, A. Jungclaus, Y. Shimizu, G. S. Simpson, P.-A. Söderström, H. Watanabe, F. Browne, P. Doornenbal et al., Phys. Rev. Lett. **114**, 192501 (2015).

[5] J. Wu, S. Nishimura, G. Lorusso, P. Möller, E. Ideguchi, P.-H. Regan, G. S. Simpson, P.-A. Söderström, P. M. Walker, H. Watanabe et al., Phys. Rev. Lett. **118**, 072701 (2017).

[6] T. Yoshida and A. L. Nichols, Assessment of Fission Product Decay Data for Decay Heat Calculations: A Report by the Working Party on International Evaluation Co-operation of the Nuclear Energy Agency Nuclear Science Committee (Nuclear Energy Agency, Organization for Economic Co-operation and Development, Paris, France, 2007).

[7] G. Mention, M. Fechner, T. Lasserre, T. A. Mueller, D. Lhuillier, M. Cribier, and A. Letourneau, Phys. Rev. D **83**, 073006 (2011).

[8] M. Fallot, S. Cormon, M. Estienne, A. Algora, V. M. Bui, A. Cucoanes, M. Elnimr, L. Giot, D. Jordan, J. Martino et al., Phys. Rev. Lett. **109**, 202504 (2012).

[9] F. P. An, A. B. Balantekin, H. R. Band, M. Bishai, S. Blyth, D. Cao, G. F. Cao, J. Cao, Y. L. Chan, J. F. Chang et al. (Daya Bay Collaboration), Phys. Rev. Lett. **118**, 251801 (2017)..

[10] P. Möller, B. Pfeiffer, and K.-L. Kratz, Phys. Rev. C **67**, 055802 (2003).

[11] M. T. Mustonen and J. Engel, Phys. Rev. C **93**, 014304 (2016).

[12] J. C. Hardy, L. C. Carraz, B. Jonson, and P. G. Hansen, Phys. Lett. **71B**, 307 (1977).

[13] E. Valencia, J. L. Tain, A. Algora, J. Agramunt, E. Estevez, M. D. Jordan, B. Rubio, S. Rice, P. Regan, W. Gelletly et al., Phys. Rev. C **95**, 024320 (2017).

[14] B. C. Rasco, K. P. Rykaczewski, A. Fijałkowska, M. Karny, M. Wolińska-Cichocka, R. K. Grzywacz, C. J. Gross, D. W. Stracener, E. F. Zganjar, J. C. Blackmon et al., Phys. Rev. C **95**, 054328 (2017).

[15] T. Yoshida and R. Nakasima, J. Nucl. Sci. Technol. **18**, 393 (1981).

[16] R. C. Greenwood, D. A. Struttmann, and K. D. Watts, Nucl. Instrum. Methods Phys. Res., Sect. A **317**, 175 (1992).

[17] M. Karny, J. M. Nitschke, L. F. Archambault, K. Burkard, D. Cano-Ott, M. Hellström, W. Hüller, R. Kirchner, S. Lewandowski, E. Roeckl et al., Nucl. Instrum. Methods Phys. Res., Sect. B **126**, 411 (1997).

[18] A. Algora, D. Jordan, J. L. Tain, B. Rubio, J. Agramunt, A. B. Perez-Cerdan, F. Molina, L. Caballero, E. Nácher, A. Krasznahorkay et al., Phys. Rev. Lett. **105**, 202501 (2010).

[19] M. Karny, K. P. Rykaczewski, A. Fijałkowska, B. C. Rasco, M. Wolińska-Cichocka, R. K. Grzywacz, K. C. Goetz, D. Miller, and E. F. Zganjar, Nucl. Instrum. Methods Phys. Res., Sect. A **836**, 83 (2016).

[20] B. C. Rasco, M. Wolińska-Cichocka, A. Fijałkowska, K. P. Rykaczewski, M. Karny, R. K. Grzywacz, K. C. Goetz, C. J. Gross, D. W. Stracener, E. F. Zganjar et al., Phys. Rev. Lett. **117**, 092501 (2016).

[21] Y. Abe, J. C. dos Anjos, J. C. Barriere, E. Baussan, I. Bekman, M. Bergevin, T. J. C. Bezerra, L. Bezrukov, E. Blucher, C. Buck et al., J. High Energy Phys. 10 (2014) 086.

[22] F. P. An, J. Z. Bai, A. B. Balantekin, H. R. Band, D. Beavis, W. Beriguete, M. Bishai, S. Blyth, K. Boddy, R. L. Brown et al., Phys. Rev. Lett. **108**, 171803 (2012).

[23] F. P. An, A. B. Balantekin, H. R. Band, M. Bishai, S. Blyth, I. Butorov, D. Cao, G. F. Cao, J. Cao, W. R. Cen et al. (Daya Bay Collaboration), Phys. Rev. Lett. **116**, 061801 (2016).

[24] J. K. Ahn, S. Chebotaryov, J. H. Choi, S. Choi, W. Choi, Y. Choi, H. I. Jang, J. S. Jang, E. J. Jeon, I. S. Jeong *et al.* (RENO Collaboration), Phys. Rev. Lett. **108**, 191802 (2012).

[25] T. A. Mueller, D. Lhuillier, M. Fallot, A. Letourneau, S. Cormon, M. Fechner, L. Giot, T. Lasserre, J. Martino, G. Mention *et al.*, Phys. Rev. C **83**, 054615 (2011).

[26] J. R. Beene, D. W. Bardayan, A. Galindo-Uribarri, C. J. Gross, K. L. Jones, J. F. Liang, W. Nazarewicz, D. W. Stracener, B. A. Tatum, and R. L. Varner, J. Phys. G **38**, 024002 (2011).

[27] D. W. Stracener, G. D. Alton, R. L. Auble, J. R. Beene, P. E. Mueller, and J. C. Bilheux, Nucl. Instrum. Methods Phys. Res., Sect. A **521**, 126 (2004).

[28] XIA LLC, *Dgital Gamma Finder (DGF) Pixie-16, Version 1.40* (XIA LLC, Hayward CA, 2009).

[29] R. Grzywacz, Nucl. Instrum. Methods Phys. Res., Sect. B **204**, 649 (2003).

[30] R. Grzywacz, C. J. Gross, A. Korgul, S. N. Liddick, C. Mazzocchi, R. D. Page, and K. Rykaczewski, Nucl. Instrum. Methods Phys. Res., Sect. B **261**, 1103 (2007).

[31] J. Allison, K. Amako, J. Apostolakis, H. Araujo, P. Dubois, M. Asai, G. Barrand, R. Capra, S. Chauvie, R. Chytracek *et al.*, IEEE Trans. Nucl. Sci. **53**, 270 (2006).

[32] J. L. Tain and D. Cano-Ott, Nucl. Instrum. Methods Phys. Res., Sect. A **571**, 728 (2007).

[33] P. K. Joshi, B. Singh, S. Singh, and A. K. Jain, Nucl. Data Sheets **138**, 1 (2016).

[34] A. Strumia and F. Vissani, Phys. Lett. B **564**, 42 (2003).

[35] M. B. Chadwick, M. Herman, P. Oblozinsky, M. E. Dunn, Y. Danon, A. C. Kahler, D. L. Smith, B. Pritychenko, G. Arbanas, R. Arcilla *et al.*, Nucl. Data Sheets **112**, 2887 (2011).

[36] JEFF-3.1 Evaluated Data Library, https://www.oecd-nea.org/dbforms/data/eva/evatapes/jeff_31/.

[37] R. Greenwood, R. Helmer, M. Putnam, and K. Watts, Nucl. Instrum. Methods Phys. Res., Sect. A **390**, 95 (1997).

[38] A.-A. Zakari-Issoufou, M. Fallot, A. Porta, A. Algora, J. L. Tain, E. Valencia, S. Rice, V. M. Bui, S. Cormon, M. Estienne *et al.* (IGISOL Collaboration), Phys. Rev. Lett. **115**, 102503 (2015).

[39] A. Tobias, Central Electricity Generating Board Report No. RD/B/6210/R89, 1989.

[40] A. A. Sonzogni, T. D. Johnson, and E. A. McCutchan, Phys. Rev. C **91**, 011301 (2015).

[41] D. A. Dwyer and T. J. Langford, Phys. Rev. Lett. **114**, 012502 (2015).

[42] I. C. Gauld, G. Radulescu, G. Ilas, B. D. Murphy, M. L. Williams, and D. Wiarda, Nuclear Technology **174**, 169 (2011).

[43] A. C. Hayes, J. L. Friar, G. T. Garvey, G. Jungman, and G. Jonkmans, Phys. Rev. Lett. **112**, 202501 (2014).

[44] P. Huber, Phys. Rev. C **84**, 024617 (2011).